

# Magnetic Properties and Magnetocaloric Effect in Ordered Double Perovskites $\text{Sr}_{1.8}\text{Pr}_{0.2}\text{FeMo}_{1-x}\text{W}_x\text{O}_6$

Imad Hussain<sup>1</sup>, Mohammad Shafique Anwar<sup>1,2</sup>, Saima Naz Khan<sup>3</sup>,  
Chan Gyu Lee<sup>1</sup> and Bon Heun Koo<sup>1†</sup>

<sup>1</sup>School of Materials Science and Engineering, Changwon National University,  
Changwon, Gyeongnam 51140, Republic of Korea

<sup>2</sup>Department of Kulliyat, A. K. T. College, Aligarh Muslim University, Aligarh, 202002, India

<sup>3</sup>Department of Physics, Abdul Wali Khan University Mardan, Pakistan

(Received April 26, 2018 : Revised July 16, 2018 : Accepted July 27, 2018)

**Abstract** We report the structural, magnetic and magnetocaloric properties of  $\text{Sr}_{1.8}\text{Pr}_{0.2}\text{FeMo}_{1-x}\text{W}_x\text{O}_6$  ( $0.0 \leq x \leq 0.4$ ) samples prepared by the conventional solid state reaction method. The X-ray diffraction analysis confirms the formation of the tetragonal double perovskite structure with a  $I4/mmm$  space group in all the synthesized samples. The temperature dependent magnetization measurements reveal that all the samples go through a ferromagnetic to paramagnetic phase transition with an increasing temperature. The Arrott plot obtained for each synthesized sample demonstrates the second order nature of the magnetic phase transition. A magnetic entropy change is obtained from the magnetic isotherms. The values of maximum magnetic entropy change and relative cooling power at an applied field of 2.5 T are found to be  $0.40 \text{ Jkg}^{-1}\text{K}^{-1}$  and  $69 \text{ Jkg}^{-1}$  respectively for the  $\text{Sr}_{1.8}\text{Pr}_{0.2}\text{FeMo}_6$  sample. The tunability of magnetization and excellent magnetocaloric features at low applied magnetic field make these materials attractive for use in magnetic refrigeration technology.

**Key words** double perovskites, magnetization, magnetocaloric effect, magnetic entropy change.

## 1. Introduction

Ambient temperature magnetic refrigeration(MR) technology challenges the existing classical gas compression technology by offering several advantages like low power consumption, stability, non-toxicity and eco-compatibility.<sup>1)</sup> MR technology is based on a well known physical phenomenon called magnetocaloric effect(MCE). The MCE is the tendency of certain materials such as paramagnetic salts or ferromagnetic substances, to heat up when placed in a magnetic field and cool down when removed from the field.<sup>2-4)</sup> The magnetocaloric parameters which distinguish a magnetic material for use in magnetic refrigeration technology include the large magnetic entropy change, large adiabatic temperature change and high relative cooling power. Although MR has a potential to increase energy efficiency of existing cooling technologies, the search for the novel room temperature magnetic

coolants working in low applied magnetic field is still an important goal to be pursued. In the search for obtaining room temperature magnetic refrigerants, several families of magnetic materials have been explored for their magnetic and magnetocaloric properties.<sup>5-7)</sup> Among the magnetic materials with potential for magnetic refrigeration, the double perovskite materials with the general formula  $\text{A}_2\text{BB}'\text{O}_6$  (A is an alkaline earth or rare earth metal atom and B, B' are the transition metal atoms) have attracted much attention due to their structural flexibilities, cationic ordering, large working temperature range and tunable transition temperatures.<sup>8-17)</sup> Rich physical properties of these materials related with the MCE have been mostly explained in terms of the ferromagnetic double exchange interaction, anti-ferromagnetic super exchange interaction, the spin phonon coupling and the strong competition between the steric effect and the electronic effect.<sup>13,18,19)</sup> Various studies have shown that B-O-B' bond angle, B/

<sup>†</sup>Corresponding author

E-Mail : [bhkoo@changwon.ac.kr](mailto:bhkoo@changwon.ac.kr) (B. H. Koo, Changwon Nat'l Univ.)

© Materials Research Society of Korea, All rights reserved.

This is an Open-Access article distributed under the terms of the Creative Commons Attribution Non-Commercial License (<http://creativecommons.org/licenses/by-nc/3.0>) which permits unrestricted non-commercial use, distribution, and reproduction in any medium, provided the original work is properly cited.

B'-O bond length, charge ordering and the oxygen deficiency are the important parameters which strongly influence the above mentioned interactions and hence the MCE in these materials. Thus it is very important to investigate these parameters when evaluating the MCE of the magnetic materials.; Besides, it is also important to explore new magnetocaloric materials which can work in a wide temperature range and with a high cooling efficiency at low cost.

In this work, we investigated the effect of partial substitution of Mo by W in the double perovskite  $\text{Sr}_{1.8}\text{Pr}_{0.2}\text{FeMo}_{1-x}\text{W}_x\text{O}_6$  ( $0.0 \leq x \leq 0.4$ ) (SPFMWO). Special focus was given to the possible modification in the structural, magnetic and magnetocaloric properties of the  $\text{Sr}_{1.8}\text{Pr}_{0.2}\text{FeMoO}_6$  (SPFMO).

## 2. Experimental Procedure

Polycrystalline SPFMWO samples were prepared by the conventional ceramic method, using high purity powders (99.9%) of  $\text{SrCO}_3$ ,  $\text{Pr}_6\text{O}_{11}$ ,  $\text{Fe}_2\text{O}_3$ ,  $\text{MoO}_3$  and  $\text{WO}_3$  as precursors. The powders were mixed, ground and then heated at  $1100^\circ\text{C}$  for 7 h in air. The mixtures obtained were re-ground and pressed into pellets at  $3\text{ t/cm}^2$ . The pellets were finally heated at  $1180^\circ\text{C}$  for 4 h under flowing 5%  $\text{H}_2$  in Ar. The phase purity and crystal structure of the obtained products were investigated by X-ray diffractometer (Bruker D8 Advance) equipped with  $\text{Cu-K}\alpha$  radiation source ( $\lambda = 1.5406\text{ \AA}$ ). The surface morphology was checked by the scanning electron microscopy (SEM, JSM 5610). The magnetic field and temperature dependent magnetization measurements were performed using a vibrating sample magnetometer (VSM; Quantum Design PPMS-6000). The magnetic isotherms were obtained at small temperature intervals near  $T_C$  under applied magnetic field up to 2.5 T.

## 3. Results and Discussion

The room temperature XRD profiles of the SPFMO samples are displayed in Fig. 1. The XRD patterns of all the samples consistently revealed the formation of the tetragonal structure with  $I4/mmm$  space group. These results are in good agreement with the JCPDS No. 72-6394. The pure double perovskite phase was achieved only in the pristine  $\text{Sr}_{1.8}\text{Pr}_{0.2}\text{FeMoO}_6$  sample. However, all the W-doped samples showed a small impurity peak of  $\text{SrMoO}_4$  (JCPDS No. 85-0809). During the formation of the double perovskite phase, the  $\text{SrMoO}_4$  impurity peak usually appears due to the incomplete reduction of the precursors in the final sintering process.<sup>20-22</sup> The superstructure reflection which gives an estimation of the cationic ordering was clearly observed at  $2\theta = 19^\circ$  in the

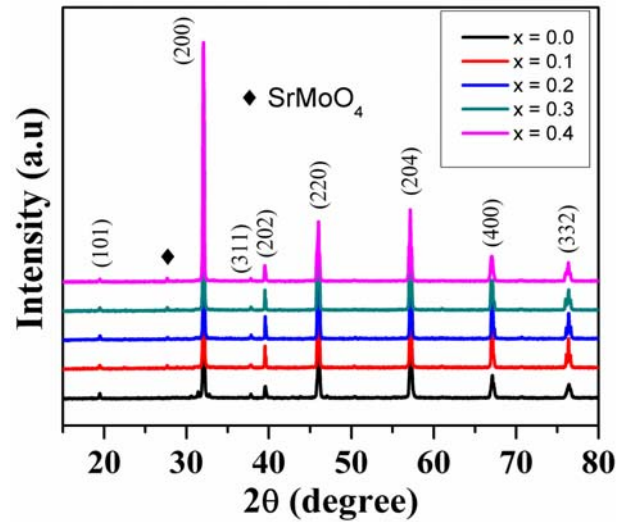


Fig. 1. Room temperature XRD patterns of  $\text{Sr}_{1.8}\text{Pr}_{0.2}\text{FeMo}_{1-x}\text{W}_x\text{O}_6$  ( $0.0 \leq x \leq 0.4$ ) samples.

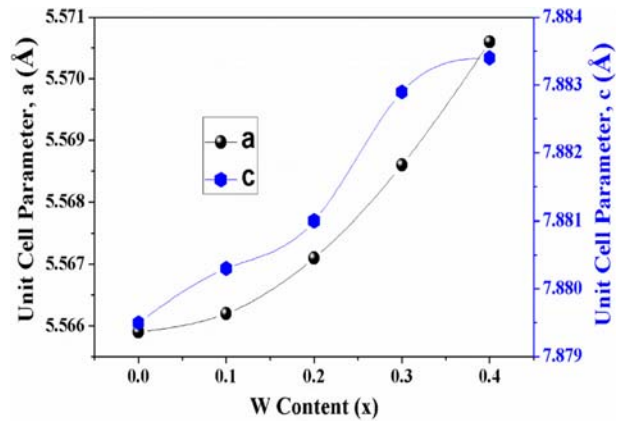
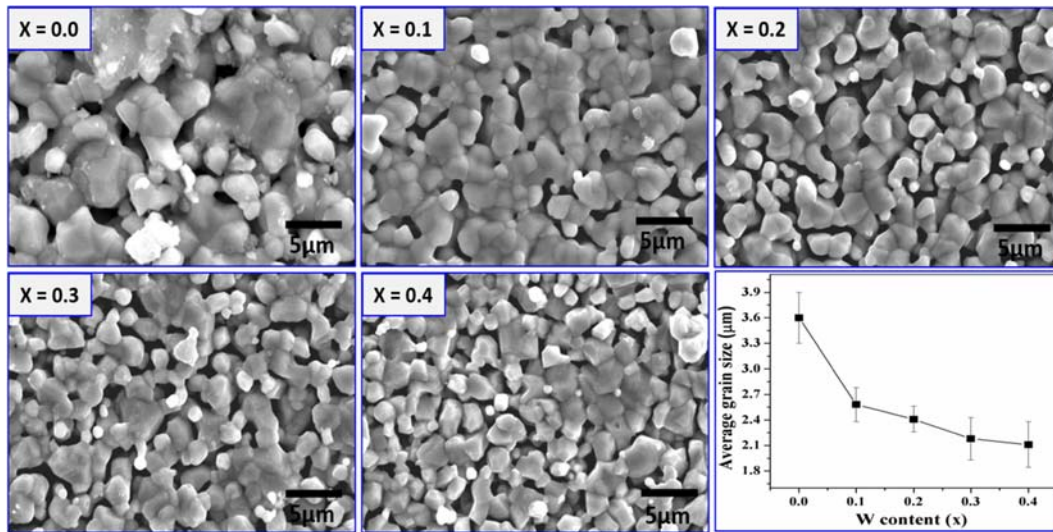
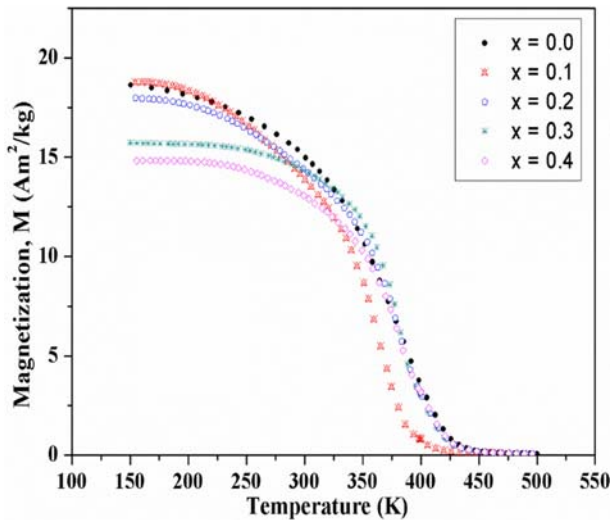


Fig. 2. The lattice parameters as a function of W-doping in  $\text{Sr}_{1.8}\text{Pr}_{0.2}\text{FeMo}_{1-x}\text{W}_x\text{O}_6$  ( $0.0 \leq x \leq 0.4$ ) samples.

XRD profiles of all the samples. The lattice parameters for the whole series were estimated using POWDER-X software. The obtained lattice parameters “a” and “c” as a function of W-doping were plotted in Fig. 2. The increase in lattice parameters with the increasing W-content is obvious due to the difference in ionic radii of  $\text{Mo}^{6+}$  (0.59 Å) and  $\text{W}^{6+}$  (0.60 Å). The microstructure and surface morphology of the samples were analyzed by SEM and the obtained images are shown in Fig. 3. Clear grain boundaries were observed in all the samples. The porosity increased with increasing W-content, suggesting that the sinterability of the SPFMO sample was decreased with increasing W-doping. However, the grain size decreased slightly with the increasing W-doping which is attributed to the relatively high melting point of  $\text{WO}_3$  as compared to  $\text{MoO}_3$ . The average grain size was estimated



**Fig. 3.** SEM images and the variation in average grain size as a function of W concentration in  $\text{Sr}_{1.8}\text{Pr}_{0.2}\text{FeMo}_{1-x}\text{W}_x\text{O}_6$  ( $0.0 \leq x \leq 0.4$ ) samples.



**Fig. 4.** Temperature dependent magnetization measured at an applied field of 0.1 T for the  $\text{Sr}_{1.8}\text{Pr}_{0.2}\text{FeMo}_{1-x}\text{W}_x\text{O}_6$  ( $0.0 \leq x \leq 0.4$ ) samples.

by image-J software and was found to be 3.6, 2.58, 2.41, 2.18 and 2.11 for  $x=0.0$ , 0.1, 0.2, 0.3 and 0.4 composition respectively.

The evolution of magnetization with respect to temperature ( $M-T$ ) for all the samples under an applied field of 0.1 T is shown in Fig. 4. Upon increasing temperature, the samples went through a ferromagnetic to paramagnetic (FM-PM) phase transition at their respective Curie temperatures ( $T_C$ ). The  $T_C$  for each sample was obtained from the minimum of the first derivative of magnetization with respect to temperature ( $dM/dT$ ). No significant change was observed in the value of  $T_C$  with increasing W-doping. Also up to  $x=0.2$ , an almost similar magnetization was observed. The competing interaction between the double

exchange interaction and the super exchange interaction may possibly lead to the almost similar magnetization behavior both in the pristine sample and the W-doped samples (up to  $x=0.2$ ). However, for increased W-doping ( $x \geq 0.3$ ), the magnetization reduced slightly. This reduction in magnetization may be attributed to the increased cation disorder in these samples.<sup>23)</sup> Moreover, due to the slightly larger ionic radius of 'W' as compared to that of 'Mo', it is anticipated here that upon increasing the W-content, the orbital hybridization and hence the exchange interaction between the Fe and Mo/W is decreased. Thus the decreased exchange interaction due to the reduced orbital hybridization may have led to the decrease in magnetization in the heavily doped ( $x \geq 0.3$ ) samples.

In order to investigate the magnetic field dependent magnetization of the samples and to confirm the ferromagnetic nature, the isothermal magnetization curves ( $M-H$ ) of the SPFMWO ( $x=0.0, 0.1, 0.3$ ) samples were obtained and are shown in Fig. 5. These isotherms were measured in the vicinity of  $T_C$  and also well above and below the  $T_C$  under an applied field varying from 0 to 2.5 T. With the increase in applied magnetic field, all the samples were observed to pass from a low magnetized state to a highly magnetized state. This variation in magnetization with the applied field was much significant at low temperatures. The rapid change in magnetization with a small change in applied field ( $H < 0.5$  T) indicated the displacement of Bloch walls. At temperatures above  $T_C$ , a much reduction in magnetization was observed. In the paramagnetic state, the pristine SPFMWO sample showed an almost linear change in magnetization with the applied magnetic field. However, the W-doping strongly influenced the behavior of the samples in paramagnetic

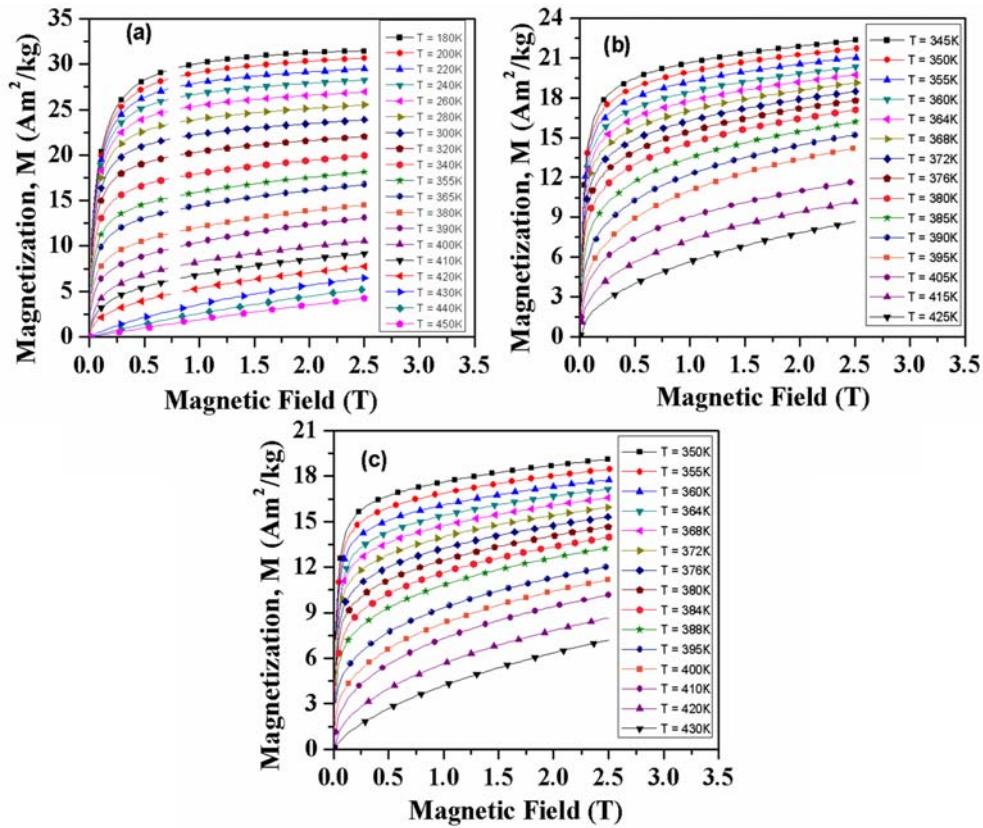


**Fig. 5.** The isothermal magnetization curves versus applied magnetic field up to 2.5 T for the  $\text{Sr}_{1.8}\text{Pr}_{0.2}\text{FeMo}_{1-x}\text{W}_x\text{O}_6$  samples (a)  $x=0.0$ , (b)  $x=0.1$ , (c)  $x=0.3$ .

state. At elevated temperatures the magnetic isotherms for the W-doped samples are not linear with the applied field in the paramagnetic region. This shows the existence of small ferromagnetic clusters at high temperature.<sup>24)</sup> The nature of the magnetic phase transition occurring in these samples was investigated by using Banerjee's criteria. According to Banerjee's criterion,<sup>25)</sup> the slopes of  $H/M$  vs.  $M^2$  curves (Arrott plots) are positive for a second order transition and negative for a first order of magnetic phase transition. In the present work, the Arrott plots for the investigated SPFMWO ( $x=0.0, 0.1, 0.3$ ) samples were obtained and are displayed in Fig. 6. At temperatures well above and below  $T_C$  in the low field region, the Arrott curves are moved in two opposite directions indicating the typical FM-PM phase transition occurring in these samples. Comparing with Banerjee's criteria, the positive slopes of the Arrott plots observed for all the samples clearly indicated the second order nature of magnetic phase transition in these samples.

In order to investigate the magnetocaloric effect (MCE) of the investigated samples, the magnetic entropy change due to the applied magnetic field can be evaluated from the M-H plots using the Maxwell relation,

$$\begin{aligned} \Delta S_m(T, H) &= S_m(T, H) - S_m(T, 0) = \int_0^H \left( \frac{\partial S}{\partial H} \right)_T dH \\ &= \int_0^H \left( \frac{\partial M}{\partial T} \right)_H dH \end{aligned} \quad (1)$$

For the magnetization recorded at discrete field and temperature intervals, the value of magnetization can be well approximated by:

$$\Delta S_m(T, H) = \sum \frac{M_i - M_{i+1}}{T_{i+1} - T_i} \Delta H_i \quad (2)$$

where  $T_i$  and  $T_{i+1}$  are the magnetization values at temperatures  $T_i$  and  $T_{i+1}$  respectively at an applied field of  $H_i$ . Using eq. 2, the MCE in terms of the magnetic entropy change ( $\Delta S_m$ ) for the synthesized samples as a function of temperature and applied magnetic field was obtained. Fig. 7 shows the magnetic entropy change versus temperature for the SPFMWO ( $x=0.0, 0.1, 0.3$ ) samples under applied field of up to 2.5 T. For each sample, the maximum magnetic entropy change was observed near  $T_C$ , where the maximum change in magnetization with temperature occurred. Further, the peak magnitude of the magnetic entropy increased with the increase in applied magnetic field. However, the peak



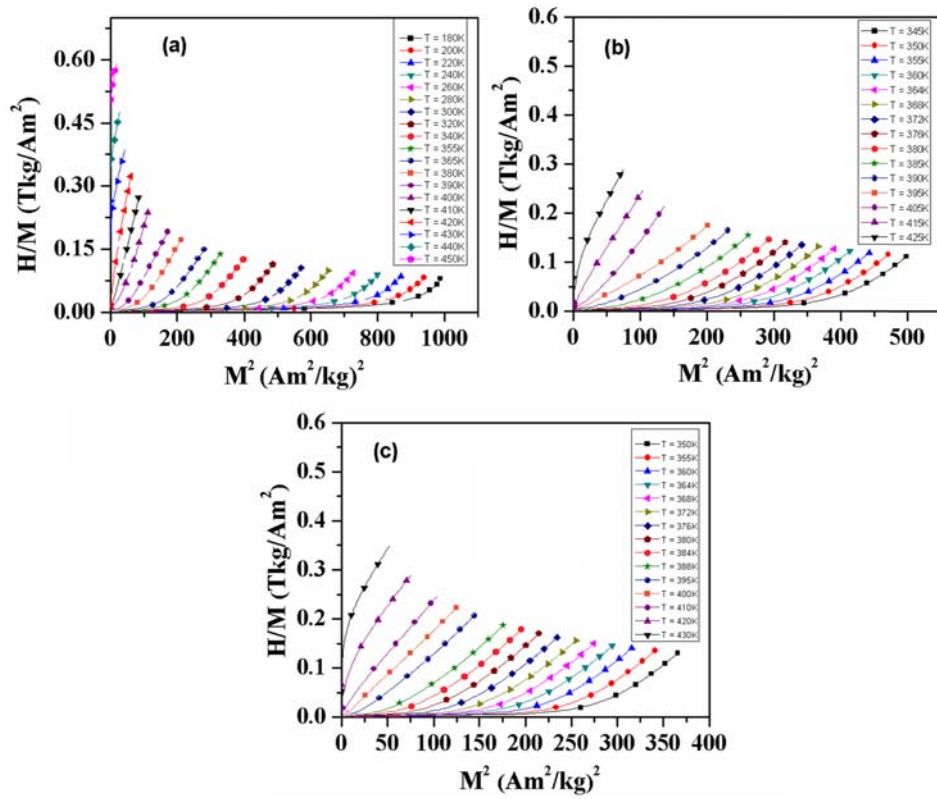


Fig. 6. Arrott plots ( $H/M$  vs.  $M^2$ ) for  $\text{Sr}_{1.8}\text{Pr}_{0.2}\text{FeMo}_{1-x}\text{W}_x\text{O}_6$  samples (a)  $x = 0.0$ , (b)  $x = 0.1$ , (c)  $x = 0.3$ .

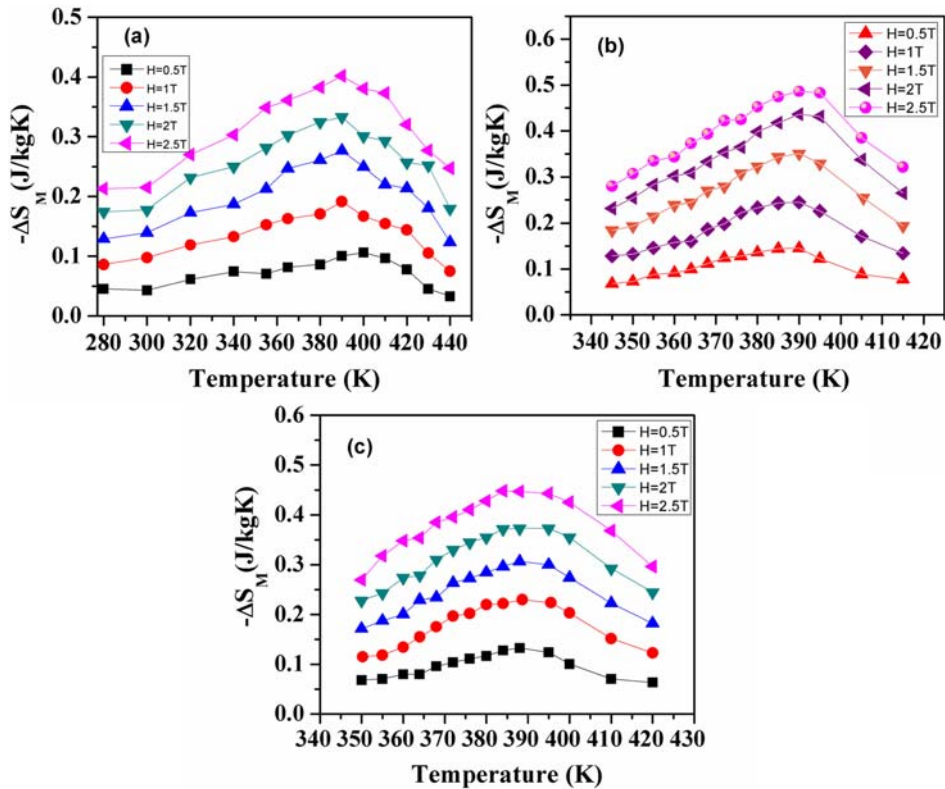
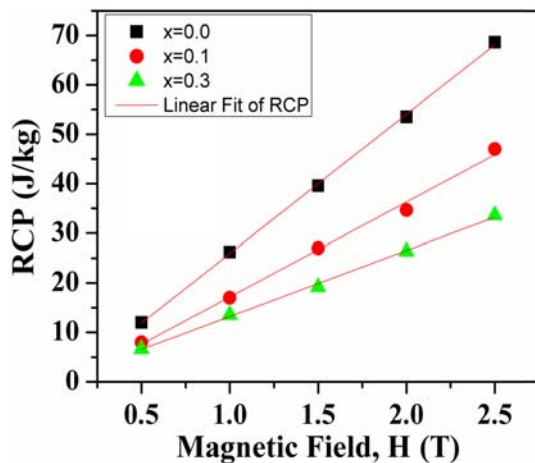


Fig. 7. Temperature dependence of magnetic entropy change measured under different applied magnetic fields for  $\text{Sr}_{1.8}\text{Pr}_{0.2}\text{FeMo}_{1-x}\text{W}_x\text{O}_6$  samples (a)  $x = 0.0$ , (b)  $x = 0.1$ , (c)  $x = 0.3$ .



**Fig. 8.** Magnetic field dependence of the relative cooling power(RCP) for the  $\text{Sr}_{1.8}\text{Pr}_{0.2}\text{FeMo}_{1-x}\text{W}_x\text{O}_6$  samples (a)  $x = 0.0$ , (b)  $x = 0.1$ , (c)  $x = 0.3$ .

position remained unchanged due to the second order nature of the magnetic phase transition. In addition to large ( $\Delta S_m$ ) value, a magnetic refrigerant is also desired to have high value of relative cooling power(RCP). The RCP of a magnetic material refers to the amount of heat per kilogram transferred between the cold and hot reservoirs during a complete refrigeration cycle. The RCP values were obtained using the relation:

$$RCP = -\Delta S_m(T, H) \times \delta T_{FWHM} \quad (3)$$

where  $\delta T_{FWHM} = T_{hot} - T_{cold}$  is the difference of temperature at the full width at half maximum of the ( $\Delta S_m$ ) curve. The RCP values obtained for the SPFMWO ( $x = 0.0, 0.1, 0.3$ ) samples are plotted in Fig. 8. A moderate increase in the RCP values was observed with the increase in applied magnetic field. The maximum value of RCP(J/kg) was observed for the pristine SPFMWO sample. In case of the W-doped samples, the RCP value was observed to decrease with increasing W-doping which is attributed to the gradual decrease in the  $\delta T_{FWHM}$ . The present work shows that the pristine SPFMWO sample can be customized for use in magnetic refrigeration technology. Further, the findings of the present work will provide a base for exploring the new magnetocaloric materials.

#### 4. Conclusions

We have investigated the effect of W-doping at the Mo-site on the structural, magnetic and magnetocaloric properties of SPFMWO samples. The samples were prepared from cheap raw materials using a simple fabrication process making them economically attractive for near room tem-

perature applications. The room temperature XRD results confirmed the formation of tetragonal double perovskite structure in all the samples. The temperature dependent magnetization measurements revealed a ferromagnetic to paramagnetic phase transition upon increasing temperature. The isothermal magnetization curves obtained for the investigated samples further verified the ferromagnetic nature of the samples at temperatures below  $T_c$ . Arrott plots obtained from the isothermal magnetization curves clearly showed the second order nature of the magnetic phase transition in all the samples. The magnetic entropy change was obtained from the isothermal magnetization curves. Though, the RCP value was observed to decrease with increasing W-doping, the simple and easily reproducible synthesis, broad magnetic entropy curves and reversible magnetocaloric effect observed in the investigated samples make them attractive for use in magnetic refrigeration technology.

#### Acknowledgement

This research was supported by Changwon National University in 2017~2018.

#### References

1. P. T. Phong, N. V. Dang, P. H. Nam, L. T. H. Phong, D. H. Manh, N. M. An and In-Ja Lee, *J. Alloys Compd.* **683**, 67 (2016).
2. M. S. Anwar, F. Ahmed, S. R. Lee, R. Danish and B. H. Koo, *Jpn. J. Appl. Phys.*, **52**, 10MC12 (2013).
3. A. Selmi, R. M'nassri, W. Cheikhrouhou-Koubaa, N. Chniba Boudjada and A. Cheikhrouhou, *J. Alloys Compd.*, **619**, 626 (2014).
4. A. G. Gamzatov, A. M. Aliev and A. R. Kaul, *J. Alloys Compd.*, **710**, 292 (2017).
5. B. G. Shen, J. R. Sun, F. X. Hu, H. W. Zhang and Z. H. Cheng, *Adv. Mater.*, **21**, 4545 (2009).
6. B. Uthaman, G. R. Raji, S. Thomas, K. G. Suresh and M. R. Varma, *J. Appl. Phys.*, **117**, 013910 (2015).
7. M. Ovichi, H. Elbidweihy, E. D. Torre, et al., *J. Appl. Phys.*, **117**, 17D107 (2015).
8. I. Hussain, M. S. Anwar, J. W. Kim, K. C. Chung and B. H. Koo, *Ceram. Int.*, **42**, 13098 (2016).
9. K. I. Kobayashi, T. Kimura, H. Sawada, K. Terakura and Y. Tokura, *Nature.*, **395**, 677 (1998).
10. J. B. Philipp, P. Majewski, L. Alff, A. Erb and R. Gross, *Phys. Rev. B.*, **68**, 144431 (2003).
11. A. H. Habib, A. Saleem, C. V. Tomy and D. Bahadur, *J. Appl. Phys.*, **97**, 10A906-1 (2005).
12. M. Musa Saad H-E, *Mater. Chem. Phys.*, **145**, 36 (2014).
13. I. Hussain, M. S. Anwar, S. N. Khan, J. W. Kim, K. C. Chung and Bon Heun Koo, *J. Alloys Compd.* **694**, 815 (2017).

14. C. Frontera, D. Rubi, J. Navarro, J. L. García-Muñoz and J. Fontcuberta, *Phys. Rev. B.*, **68**, 012412 (2003).
15. D. Rubi, C. Frontera, G. Herranz, J.L.G. Muñoz, J. Fontcuberta and C. Ritter, *J. Appl. Phys.*, **95**, 7082 (2004).
16. A. K. Azad, S. G. Eriksson, K. Abdullah, A. Riksson and M. Tsegai, *J. Solid State Chem.*, **179**, 1303 (2006).
17. E. K. Hemery, G. V. M. Williams and H. J. Trodahl, *Phys. Rev. B.*, **74**, 054423 (2006).
18. D. D. Sarma, P. Mahadevan, T. Saha-Dasgupta, S. Ray and A. Kumar, *Phys. Rev. Lett.*, **85**, 2549 (2000).
19. J. Navarro, C. Frontera, L. I. Balcells, B. Martínez and J. Fontcuberta, *Phys. Rev. B.*, **64**, 092411 (2001).
20. Q. Zhang, T. Wei and Yun-Hui Huang, *J. Power Sources*, **198**, 59 (2012).
21. F. Sriti, N. Nguyen, C. Martin, A. Ducouret and B. Raveau, *J. Magn. Magn. Mater.*, **250**, 123 (2002).
22. A. K. Azad, S. -G. Eriksson, S. A. Ivanov, R. Mathieu, P. Svedlindh, J. Eriksen and H. Rundlof, *J. Alloys Compd.*, **364**, 77 (2004).
23. Q. Zhang, Z. F. Xu, H. B. Sun, X. Zhang, H. Wang and G. H. Rao, *J. Alloys Compd.*, **745**, 525 (2018).
24. M. Bourouina, A. Krichene, N. Chniba Boudjada, M. Khitouni and W. Boujelben, *Ceram. Int.*, **43**, 8139 (2017).
25. B. K. Banerjee, *Phys. Lett.*, **12**, 16 (1964).